

A. Theoretical Analysis

Assumptions. To derive the sequel propositions and theorems, we first introduce a general assumption about the smoothness of $-\log q_\phi(\mathbf{x})$ and $-\log c_\theta(\mathbf{z}, \mathbf{y})$, that is, these two log-likelihood functions are assumed to be continuous differentiable, and their gradients are L -Lipschitz continuous.

A.1. Proof of Theorem 1

First, we show that the gap between the proximal operators is bounded above.

Proof of Theorem 1. For the one diffusion reverse step, the hyperparameter δ_t is equal to $\delta + \frac{L}{2} \left(\frac{Q_f - 1}{Q_f + 1} \right)^2 \|\mathbf{x}_t - \tilde{\mathbf{x}}_0\|^2$. Because $-\log q_\phi$ is L -smooth, then we know that $\mathbf{x} \rightarrow -\log q_\phi(\mathbf{x}) + \frac{\rho}{2} \|\mathbf{x} - \hat{\mathbf{x}}_t\|^2$ is $(\rho - L)$ -strongly convex and $(\rho + L)$ -smooth. Note that $\mathbf{x}_{t-1} = \mathbf{x}_t - \eta \nabla h_t(\mathbf{x}_t)$, then by the standard convex optimization theory [38], we have

$$-\log q_\phi(\mathbf{x}_{t-1}) + \frac{\rho}{2} \|\mathbf{x}_{t-1} - \hat{\mathbf{x}}_t\|^2 \leq -\log q_\phi(\hat{\mathbf{x}}) + \frac{\rho}{2} \|\hat{\mathbf{x}} - \hat{\mathbf{x}}_t\|^2 + \frac{L}{2} \left(\frac{Q_f - 1}{Q_f + 1} \right)^2 \|\mathbf{x}_t - \tilde{\mathbf{x}}_0\|^2, \quad (\text{A.1})$$

where $Q_f = (\rho - L)/(\rho + L)$. Combining (A.1) and part (i), we get that

$$-\log p(\mathbf{x}_{t-1}) + \frac{\rho}{2} \|\mathbf{x}_{t-1} - \hat{\mathbf{x}}_t\|^2 \leq -\log p(\hat{\mathbf{x}}) + \frac{\rho}{2} \|\hat{\mathbf{x}} - \hat{\mathbf{x}}_t\|^2 + \delta + \frac{L}{2} \left(\frac{Q_f - 1}{Q_f + 1} \right)^2 \|\mathbf{x}_t - \tilde{\mathbf{x}}_0\|^2. \quad \square$$

A.2. Proof of Theorem 2

Before proving the convergence results of Algorithm 1, we first discuss what the limit points are if Algorithm 1 converges.

Proposition 2. Let $\{(\mathbf{x}_t, \mathbf{z}_t, \boldsymbol{\mu}_t)\}$ be the sequence generated by Algorithm 1. If $\mathbf{z}_t = \mathbf{z}_{t-1}$, $\mathbf{x}_t = \mathbf{x}_{t-1}$, $\boldsymbol{\mu}_t = \boldsymbol{\mu}_{t-1}$, holds for some t , then

$$\mathbf{x}_{t-1} = \mathbf{z}_{t-1}, \quad \nabla (\log p(\mathbf{x}_{t-1}) + \log p(\mathbf{y}|\mathbf{x}_{t-1})) = 0,$$

Hence, \mathbf{x}_{t-1} is a stationary point of the minimization problem.

Proof. According to the definition of $\boldsymbol{\mu}_t$, we have

$$\mathbf{x}_{t-1} - \mathbf{z}_{t-1} = \rho(\boldsymbol{\mu}_{t-1} - \boldsymbol{\mu}_t) = 0.$$

On the other side, $\mathbf{x}_{t-1} \in \arg \min_{\mathbf{x}} -\log p(\mathbf{x}) + \langle \mathbf{x} - \mathbf{z}_t, \boldsymbol{\mu}_t \rangle + \frac{\rho}{2} \|\mathbf{x} - \mathbf{z}_t\|^2$. Then from the first order condition, we obtain that

$$\nabla_{\mathbf{x}_{t-1}} (-\log p(\mathbf{x}_{t-1}) + \boldsymbol{\mu}_t + \rho(\mathbf{x}_{t-1} - \mathbf{z}_t)) = 0. \quad (\text{A.2})$$

Similarly, according to the definition of \mathbf{z}_{t-1} , we know that

$$\nabla_{\mathbf{z}_{t-1}} (-\log p(\mathbf{y}|\mathbf{z}_{t-1}) - \boldsymbol{\mu}_t + \rho(\mathbf{x}_{t-1} - \mathbf{z}_{t-1})) = 0. \quad (\text{A.3})$$

Combining (A.2) and (A.3), we get that

$$\nabla (-\log p(\mathbf{x}_{t-1}) - \log p(\mathbf{y}|\mathbf{x}_{t-1})) = 0. \quad \square$$

To prove Theorem 2, we first present a simplified version of the Robbins-Siegmund theorem which will be used later.

Lemma 1 ([43]). Consider a filter $\{\mathcal{F}_k\}_k$, the nonnegative sequence of $\{\mathcal{F}_k\}_k$ -adapted processes $\{V_k\}_k$, $\{U_k\}_k$, and $\{Z_k\}_k$ such that $\sum_k Z_k < +\infty$ almost surely, and

$$\mathbb{E}[V_{k+1}|\mathcal{F}_k] + U_{k+1} \leq V_k + Z_k, \quad \forall k \geq 0.$$

Then $\{V_k\}_k$ converges and $\sum_k U_k < +\infty$ almost surely.

The Robbins-Siegmund theorem provided in this paper is a stochastic version. However, we will only consider the deterministic version in the proof of Theorem 2. We now move on to the proof of Theorem 2.

Proof of Theorem 2. To adapt the formal index settings in optimization perspective, we reverse the index order in the proof. In other words, we let $\mathbf{x}_k \leftarrow \mathbf{x}_{T-k}$, $\mathbf{z}_k \leftarrow \mathbf{z}_{T-k}$, and $\boldsymbol{\mu}_k \leftarrow \boldsymbol{\mu}_{T-k}$, respectively. Moreover, to simplify the notations used in the proof, we defined $g(\mathbf{z}) := -\log c_\theta(\mathbf{z}, \mathbf{y})$ and $f(\mathbf{x}) := -\log p(\mathbf{x})$.

Step 1. Let $\mathbf{z}_{k+1}^* := \arg \min_{\mathbf{z}} \mathcal{L}(\mathbf{x}_{k+1}, \mathbf{z}, \boldsymbol{\mu}_k)$. According to the assumption of g , we have that the mapping $\mathbf{z} \rightarrow \mathcal{L}(\mathbf{x}_{k+1}, \mathbf{z}, \boldsymbol{\mu}_k)$ is $(\rho - L)$ -strongly convex and $(\rho + L)$ -smooth. Thus the gradient descent steps in Algorithm 1 show that

$$\|\mathbf{z}_{k+1} - \mathbf{z}_{k+1}^*\| \leq \left(1 - \frac{\rho - L}{\rho + L}\right)^{K_k} \|\mathbf{z}_k - \mathbf{z}_{k+1}^*\| \leq \sqrt{d} \left(\frac{2L}{\rho + L}\right)^{K_k},$$

where d is the dimension of \mathbf{z} . The last inequality holds due to the nature of \mathbf{z}_k being an image, which implies that \mathbf{z}_k belongs to the interval $[0, 1]^d$. For ease of notation, we define $\Delta_k := \sqrt{d} \left(\frac{2L}{\rho + L}\right)^{K_k}$.

On the other side, according to the definition of \mathbf{z}_{k+1}^* , we have

$$0 = \nabla g(\mathbf{z}_{k+1}^*) - \boldsymbol{\mu}_k + \rho(\mathbf{x}_{k+1} - \mathbf{z}_{k+1}^*). \quad (\text{A.4})$$

Noting that $\boldsymbol{\mu}_{k+1} = \boldsymbol{\mu}_k + \rho(\mathbf{x}_{k+1} - \mathbf{z}_{k+1})$, we get

$$\nabla g(\mathbf{z}_{k+1}^*) = \boldsymbol{\mu}_{k+1} + \rho(\mathbf{z}_{k+1} - \mathbf{z}_{k+1}^*),$$

from equation (A.4). Hence, we can obtain an upper bound of the gap between $\boldsymbol{\mu}_{k+1}$ and $\boldsymbol{\mu}_k$ by the smoothness of g ,

$$\begin{aligned} \|\boldsymbol{\mu}_{k+1} - \boldsymbol{\mu}_k\| &= \|\nabla g(\mathbf{z}_{k+1}^*) - \nabla g(\mathbf{z}_k^*) + \rho(\mathbf{z}_{k+1}^* - \mathbf{z}_{k+1}) - \rho(\mathbf{z}_k^* - \mathbf{z}_k)\| \\ &\leq \|\nabla g(\mathbf{z}_{k+1}^*) - \nabla g(\mathbf{z}_k^*)\| + \rho\|\mathbf{z}_{k+1}^* - \mathbf{z}_{k+1}\| + \rho\|\mathbf{z}_k^* - \mathbf{z}_k\| \\ &\leq L\|\mathbf{z}_{k+1}^* - \mathbf{z}_k^*\| + \rho\|\mathbf{z}_{k+1}^* - \mathbf{z}_{k+1}\| + \rho\|\mathbf{z}_k^* - \mathbf{z}_k\| \\ &\leq L(\|\mathbf{z}_{k+1}^* - \mathbf{z}_{k+1}\| + \|\mathbf{z}_{k+1} - \mathbf{z}_k\| + \|\mathbf{z}_k - \mathbf{z}_k^*\|) + \rho\|\mathbf{z}_{k+1}^* - \mathbf{z}_{k+1}\| + \rho\|\mathbf{z}_k^* - \mathbf{z}_k\| \\ &= L\|\mathbf{z}_{k+1} - \mathbf{z}_k\| + (L + \rho)\|\mathbf{z}_{k+1} - \mathbf{z}_{k+1}^*\| + (L + \rho)\|\mathbf{z}_k - \mathbf{z}_k^*\|. \end{aligned} \quad (\text{A.5})$$

Step 2. Let $\mathbf{x}_{k+1}^* := \arg \min_{\mathbf{x}} \mathcal{L}(\mathbf{x}, \mathbf{z}_k, \boldsymbol{\mu}_k)$. Because $\mathbf{x} \rightarrow \mathcal{L}(\mathbf{x}, \mathbf{z}_k, \boldsymbol{\mu}_k)$ is $(\rho - L)$ -strongly convex for all $k \geq 0$, we have

$$\frac{\rho - L}{2} \|\mathbf{x}_{k+1} - \mathbf{x}_{k+1}^*\|^2 \leq f(\mathbf{x}_{k+1}) + \frac{\rho}{2} \|\mathbf{x}_{k+1} - \mathbf{u}_k\|^2 - f(\mathbf{x}_{k+1}^*) - \frac{\rho}{2} \|\mathbf{x}_{k+1}^* - \mathbf{u}_k\|^2 \leq \delta_k.$$

Hence,

$$\|\mathbf{x}_{k+1} - \mathbf{x}_{k+1}^*\|^2 \leq \frac{2\delta_k}{\rho - L}.$$

Then,

$$\begin{aligned} \mathcal{L}(\mathbf{x}_k, \mathbf{z}_k, \boldsymbol{\mu}_k) - \mathcal{L}(\mathbf{x}_{k+1}, \mathbf{z}_k, \boldsymbol{\mu}_k) &\geq \langle \nabla_{\mathbf{x}} \mathcal{L}(\mathbf{x}_{k+1}, \mathbf{z}_k, \boldsymbol{\mu}_k), \mathbf{x}_k - \mathbf{x}_{k+1} \rangle + \frac{\rho - L}{2} \|\mathbf{x}_k - \mathbf{x}_{k+1}\|^2 \\ &\geq -\frac{1}{2} \|\nabla_{\mathbf{x}} \mathcal{L}(\mathbf{x}_{k+1}, \mathbf{z}_k, \boldsymbol{\mu}_k)\|^2 - \frac{1}{2} \|\mathbf{x}_k - \mathbf{x}_{k+1}\|^2 + \frac{\rho - L}{2} \|\mathbf{x}_k - \mathbf{x}_{k+1}\|^2 \\ &\geq -\frac{(\rho + L)\delta_k}{\rho - L} + \frac{\rho - L - 1}{2} \|\mathbf{x}_k - \mathbf{x}_{k+1}\|^2, \end{aligned}$$

where the last inequality holds because $\mathbf{x} \rightarrow \mathcal{L}(\mathbf{x}, \mathbf{z}_k, \boldsymbol{\mu}_k)$ is $(\rho + L)$ -smooth, and $\mathbf{x}_{k+1}^* := \arg \min_{\mathbf{x}} \mathcal{L}(\mathbf{x}, \mathbf{z}_k, \boldsymbol{\mu}_k)$.

Step 3. Now, we have

$$\begin{aligned}
& \mathcal{L}(\mathbf{x}_{k+1}, \mathbf{z}_k, \boldsymbol{\mu}_k) - \mathcal{L}(\mathbf{x}_{k+1}, \mathbf{z}_{k+1}, \boldsymbol{\mu}_{k+1}) \\
&= g(\mathbf{z}_k) - g(\mathbf{z}_{k+1}) + \langle \boldsymbol{\mu}_{k+1}, \mathbf{z}_{k+1} - \mathbf{z}_k \rangle + \frac{\rho}{2} \|\mathbf{z}_k - \mathbf{z}_{k+1}\|^2 - \rho \|\boldsymbol{\mu}_k - \boldsymbol{\mu}_{k+1}\|^2 \\
&= g(\mathbf{z}_k) - g(\mathbf{z}_{k+1}) + \langle \nabla g(\mathbf{z}_{k+1}^*) - \rho(\mathbf{z}_{k+1} - \mathbf{z}_{k+1}^*), \mathbf{z}_{k+1} - \mathbf{z}_k \rangle + \frac{\rho}{2} \|\mathbf{z}_k - \mathbf{z}_{k+1}\|^2 - \rho \|\boldsymbol{\mu}_k - \boldsymbol{\mu}_{k+1}\|^2 \\
&= g(\mathbf{z}_k) - g(\mathbf{z}_{k+1}) + \langle \nabla g(\mathbf{z}_{k+1}), \mathbf{z}_{k+1} - \mathbf{z}_k \rangle + \langle \nabla g(\mathbf{z}_{k+1}) - \nabla g(\mathbf{z}_{k+1}^*), \mathbf{z}_{k+1} - \mathbf{z}_k \rangle \\
&\quad + \rho \langle \mathbf{z}_{k+1}^* - \mathbf{z}_{k+1}, \mathbf{z}_{k+1} - \mathbf{z}_k \rangle + \frac{\rho}{2} \|\mathbf{z}_k - \mathbf{z}_{k+1}\|^2 - \rho \|\boldsymbol{\mu}_k - \boldsymbol{\mu}_{k+1}\|^2 \\
&\geq -\frac{L}{2} \|\mathbf{z}_k - \mathbf{z}_{k+1}\|^2 - \frac{1}{2} \|\mathbf{z}_k - \mathbf{z}_{k+1}\|^2 - \frac{L^2}{2} \|\mathbf{z}_{k+1} - \mathbf{z}_{k+1}^*\|^2 - \frac{1}{2} \|\mathbf{z}_{k+1} - \mathbf{z}_k\|^2 \\
&\quad - \frac{\rho^2}{2} \|\mathbf{z}_{k+1} - \mathbf{z}_{k+1}^*\|^2 + \frac{\rho}{2} \|\mathbf{z}_k - \mathbf{z}_{k+1}\|^2 - \frac{1}{\rho} \|\boldsymbol{\mu}_k - \boldsymbol{\mu}_{k+1}\|^2 \\
&\geq \left(\frac{\rho}{2} - \frac{L}{2} - 1 \right) \|\mathbf{z}_k - \mathbf{z}_{k+1}\|^2 - \frac{L^2 + \rho^2}{2} \|\mathbf{z}_{k+1} - \mathbf{z}_{k+1}^*\|^2 - \frac{1}{\rho} \|\boldsymbol{\mu}_k - \boldsymbol{\mu}_{k+1}\|^2 \\
&\geq \left(\frac{\rho}{2} - \frac{L}{2} - 1 \right) \|\mathbf{z}_k - \mathbf{z}_{k+1}\|^2 - \frac{L^2 + \rho^2}{2} \|\mathbf{z}_{k+1} - \mathbf{z}_{k+1}^*\|^2 \\
&\quad - \frac{3}{\rho} \left(L^2 \|\mathbf{z}_{k+1} - \mathbf{z}_k\|^2 + (L + \rho)^2 \Delta_k^2 + (L + \rho)^2 \Delta_{k-1}^2 \right) \\
&\geq \left(\frac{\rho}{2} - \frac{L}{2} - 1 - \frac{3L^2}{\rho} \right) \|\mathbf{z}_k - \mathbf{z}_{k+1}\|^2 - \left(\frac{L^2 + \rho^2}{2} \Delta_k^2 + \frac{3(L + \rho)^2}{\rho} \Delta_k^2 + \frac{3(L + \rho)^2}{\rho} \Delta_{k-1}^2 \right).
\end{aligned}$$

Step 4. In this step, we will show that the augmented Lagrangian function sequence $\{\mathcal{L}(\mathbf{x}_k, \mathbf{z}_k, \boldsymbol{\mu}_k)\}_k$ is nonincreasing. Let $\mathcal{L}_k := \mathcal{L}(\mathbf{x}_k, \mathbf{z}_k, \boldsymbol{\mu}_k)$. According to Step 2 and 3, we get that

$$\begin{aligned}
\mathcal{L}_k - \mathcal{L}_{k+1} &\geq \left(\frac{\rho}{2} - \frac{L}{2} - 1 - \frac{3L^2}{\rho} \right) \|\mathbf{z}_k - \mathbf{z}_{k+1}\|^2 + \frac{\rho - L - 1}{2} \|\mathbf{x}_k - \mathbf{x}_{k+1}\|^2 \\
&\quad - \left(\frac{L^2 + \rho^2}{2} \Delta_k^2 + \frac{3(L + \rho)^2}{\rho} \Delta_k^2 + \frac{3(L + \rho)^2}{\rho} \Delta_{k-1}^2 \right) - \frac{(\rho + L)\delta_k}{\rho - L}.
\end{aligned}$$

Because $\rho > 6L$, then there exist constants

$$c_1 := L, \quad c_2 := \frac{L^2 + \rho^2}{2} + \frac{3(L + \rho)^2}{\rho}, \quad c_3 := \frac{3(L + \rho)^2}{\rho}, \quad c_4 := \frac{(\rho + L)}{\rho - L},$$

such that

$$c_1 (\|\mathbf{z}_k - \mathbf{z}_{k+1}\|^2 + \|\mathbf{x}_k - \mathbf{x}_{k+1}\|^2) + \mathcal{L}_{k+1} \leq \mathcal{L}_k + c_2 \Delta_k^2 + c_3 \Delta_{k-1}^2 + c_4 \delta_k. \quad (\text{A.6})$$

Hence that the sequence $\{\mathcal{L}(\mathbf{x}_k, \mathbf{z}_k, \boldsymbol{\mu}_k)\}_k$ is decreasing. In the rest of this step, we will show that $\{\mathcal{L}_k\}_k$ is bounded from below. Because we assume that $\min\{f(\mathbf{z}) + g(\mathbf{x}) : \mathbf{z} = \mathbf{x}\} > -\infty$, we obtain that for all k ,

$$\begin{aligned}
\mathcal{L}(\mathbf{x}_k, \mathbf{z}_k, \boldsymbol{\mu}_k; \rho) &= f(\mathbf{x}_k) + g(\mathbf{z}_k) + \langle \boldsymbol{\mu}_k, \mathbf{x}_k - \mathbf{z}_k \rangle + \frac{\rho}{2} \|\mathbf{z}_k - \mathbf{x}_k\|^2 \\
&= f(\mathbf{x}_k) + g(\mathbf{z}_k) + \langle \nabla g(\mathbf{z}_k^*) - \rho(\mathbf{z}_k - \mathbf{z}_k^*), \mathbf{x}_k - \mathbf{z}_k \rangle + \frac{\rho}{2} \|\mathbf{z}_k - \mathbf{x}_k\|^2 \\
&= f(\mathbf{x}_k) + g(\mathbf{x}_k) + g(\mathbf{z}_k) - g(\mathbf{x}_k) + \langle \nabla g(\mathbf{z}_k), \mathbf{x}_k - \mathbf{z}_k \rangle + \frac{\rho}{2} \|\mathbf{z}_k - \mathbf{x}_k\|^2 \\
&\quad + \langle \nabla g(\mathbf{z}_k^*) - \nabla g(\mathbf{z}_k) - \rho(\mathbf{z}_k - \mathbf{z}_k^*), \mathbf{x}_k - \mathbf{z}_k \rangle \\
&\geq f(\mathbf{x}_k) + g(\mathbf{x}_k) - \frac{L}{2} \|\mathbf{x}_k - \mathbf{z}_k\|^2 + \frac{\rho}{2} \|\mathbf{z}_k - \mathbf{x}_k\|^2 - \frac{L^2 + \rho^2}{2} \|\mathbf{z}_k^* - \mathbf{z}_k\|^2 - \|\mathbf{x}_k - \mathbf{z}_k\|^2 \\
&\geq f(\mathbf{x}_k) + g(\mathbf{x}_k) - \frac{L^2 + \rho^2}{2} \|\mathbf{z}_k^* - \mathbf{z}_k\|^2 \geq \min\{f(\mathbf{z}) + g(\mathbf{z})\} - \frac{(L^2 + \rho^2)\Delta_{k-1}^2}{2}.
\end{aligned}$$

Hence, the sequence $\{\mathcal{L}(\mathbf{z}_k, \mathbf{x}_k, \boldsymbol{\mu}_k)\}_k$ is bounded from below.

Step 5. Now we will prove that $\lim_{j \rightarrow \infty} (\|\mathbf{z}_{k+1} - \mathbf{z}_k\|^2 + \|\mathbf{x}_{k+1} - \mathbf{x}_k\|^2) = 0$. For ease of notation, we define $m_k := \|\mathbf{z}_{k+1} - \mathbf{z}_k\|^2 + \|\mathbf{x}_{k+1} - \mathbf{x}_k\|^2$ for all $k = 0, 1, \dots$. Summing equation (A.6) for k from 0 to $+\infty$, we get that

$$c_1 \sum_{k=0}^{\infty} m_k \leq \mathcal{L}_0 - \inf_k \mathcal{L}_k + \sum_{k=0}^{\infty} (c_2 \Delta_k^2 + c_3 \Delta_{k-1}^2 + c_4 \delta_k).$$

On the other side, recalling the definition of Δ_k and noting that $(2L)/(\rho + L) < 1$, we get that $\sum_k \Delta_k^2 < +\infty$. Therefore, the sum of m_k for all k is finite ($\sum_k m_k < +\infty$), which implies that $\lim_{k \rightarrow \infty} m_k = 0$. Moreover, by (A.5), we get that

$$\|\boldsymbol{\mu}_k - \boldsymbol{\mu}_{k+1}\| \leq L \|\mathbf{z}_{k+1} - \mathbf{z}_k\| + (L + \rho)(\Delta_k + \Delta_{k-1}) \rightarrow 0, \quad \text{as } k \rightarrow \infty.$$

Step 6. In this part, we will show that the algorithm will converge to a stationary point of problem (P). By Step 5, we know that

$$\lim_k \|\mathbf{x}_{k+1} - \mathbf{x}_k\| = 0, \quad \lim_k \|\mathbf{z}_{k+1} - \mathbf{z}_k\| = 0, \quad \lim_k \|\boldsymbol{\mu}_{k+1} - \boldsymbol{\mu}_k\| = 0.$$

Let $(\mathbf{x}_\infty, \mathbf{z}_\infty, \boldsymbol{\mu}_\infty)$ be the limit point of the sequence. Combing with Proposition 2, we get that \mathbf{x}_∞ is a stationary point of the minimization problem (P).

Step 7. In this step, we use the Robbins-Siegmund theorem to get a refine analysis to the convergence rate of the ADMM. In particular, we prove the sublinear convergence rate. Now define for all $k \in \mathbb{N}$,

$$w_k := \frac{2}{k+1}, \quad \lambda_0 := h_0, \quad \lambda_{k+1} := (1 - w_k)\lambda_k + w_k m_k.$$

Note that if we show that $m_k \rightarrow 0$ as $k \rightarrow \infty$, we can prove that convergence of the ADMM. Now we have $w_k \in [0, 1]$, and λ_{k+1} is a convex combination of $\{m_0, \dots, m_k\}$. Rearranging equation (A.6), we have

$$\frac{(k+1)c_1}{2} \lambda_{k+1} + \mathcal{L}_{k+1} + \frac{c_1}{2} \lambda_k \leq \frac{kc_1}{2} \lambda_k + \mathcal{L}_k + c_2 \Delta_k^2 + c_3 \Delta_{k-1}^2 + c_4 \delta_k.$$

Using the Robbins-Siegmund theorem, we have the sequence $\{k\lambda_k\}_k$ converges and that $\sum_k \lambda_k < +\infty$. In particular, it implies that $\lim_{k \rightarrow \infty} \lambda_k = 0$. Note that $\lambda_k = \frac{1}{k} \cdot k\lambda_k$, then we have $\lim_{k \rightarrow \infty} k\lambda_k = 0$ because $\sum_k \lambda_k < +\infty$. Hence,

$$\lambda_k = o(k^{-1}).$$

On the other side, λ_k is a convex combination of $\{m_0, \dots, m_k\}$, then we have

$$\min_{j \in \{0, \dots, k\}} m_j \leq \lambda_k = o(k^{-1}).$$

□

B. Implementation Details

The source code is available in this [link](#).

C. Further Experimental Results

We provide additional quantitative evaluations based on the PNSR and SSIM metrics in Table 5 and Table 6.

In Figure 5, we compare the visual results of our method with GMD without trajectory inpainting.

| Method | SR ($\times 4$) | | Inpaint (box) | | Inpaint (random) | | Deblur (gauss) | | Deblur (motion) | |
|----------------|-------------------|-----------------|-----------------|-----------------|------------------|-----------------|-----------------|-----------------|-----------------|-----------------|
| | PSNR \uparrow | SSIM \uparrow | PSNR \uparrow | SSIM \uparrow | PSNR \uparrow | SSIM \uparrow | PSNR \uparrow | SSIM \uparrow | PSNR \uparrow | SSIM \uparrow |
| ADMM-TV | 23.86 | 0.803 | 17.81 | 0.814 | 22.03 | 0.784 | 22.37 | 0.801 | 21.36 | 0.758 |
| Score-SDE [50] | 17.62 | 0.617 | 18.51 | 0.678 | 13.52 | 0.437 | 7.12 | 0.109 | 6.58 | 0.102 |
| PnP-ADMM [7] | 26.55 | 0.865 | 11.65 | 0.642 | 8.41 | 0.325 | <u>24.93</u> | 0.812 | 24.65 | 0.825 |
| MCG [9] | 20.05 | 0.559 | 19.97 | 0.703 | 21.57 | 0.751 | 6.72 | 0.051 | 6.72 | 0.055 |
| DDRM [26] | 25.36 | 0.835 | 22.24 | 0.869 | 9.19 | 0.319 | 23.36 | 0.767 | - | - |
| DPS [8] | <u>25.67</u> | 0.852 | <u>22.47</u> | <u>0.873</u> | <u>25.23</u> | <u>0.851</u> | 24.25 | <u>0.811</u> | 24.92 | 0.859 |
| ADMMDiff | 28.08 | <u>0.857</u> | 22.5 | 0.878 | 33.4 | 0.930 | 25.1 | 0.794 | 25.6 | <u>0.827</u> |

Table 5. Quantitative evaluation (PSNR, SSIM) of solving linear inverse problems on FFHQ 256×256 -1k validation dataset. **Bold** indicates the best. Underline indicates the second best.

| Method | SR ($\times 4$) | | Inpaint (box) | | Inpaint (random) | | Deblur (gauss) | | Deblur (motion) | |
|----------------|-------------------|-----------------|-----------------|-----------------|------------------|-----------------|-----------------|-----------------|-----------------|-----------------|
| | PSNR \uparrow | SSIM \uparrow | PSNR \uparrow | SSIM \uparrow | PSNR \uparrow | SSIM \uparrow | PSNR \uparrow | SSIM \uparrow | PSNR \uparrow | SSIM \uparrow |
| ADMM-TV | 22.17 | 0.679 | 17.96 | 0.785 | 20.96 | 0.676 | 19.99 | 0.634 | 20.79 | <u>0.677</u> |
| Score-SDE [50] | 12.25 | 0.256 | 16.48 | 0.612 | 18.62 | 0.517 | 15.97 | 0.436 | 7.21 | 0.120 |
| PnP-ADMM [7] | 23.75 | 0.761 | 12.70 | 0.657 | 8.39 | 0.300 | 21.81 | 0.669 | 21.98 | 0.702 |
| MCG [9] | 13.39 | 0.227 | 17.36 | 0.633 | 19.03 | 0.546 | 16.32 | 0.441 | 5.89 | 0.037 |
| DDRM [26] | 24.96 | 0.790 | 18.66 | 0.814 | 14.29 | 0.403 | <u>22.73</u> | 0.705 | - | - |
| DPS [8] | 23.87 | <u>0.781</u> | 18.90 | 0.794 | <u>22.20</u> | <u>0.739</u> | 21.97 | <u>0.706</u> | <u>20.55</u> | 0.634 |
| ADMMDiff | 25.04 | 0.688 | 19.03 | 0.814 | 27.93 | 0.824 | 23.32 | 0.716 | 25.11 | 0.670 |

Table 6. Quantitative evaluation (PSNR, SSIM) of solving linear inverse problems on ImageNet 256×256 -1k validation dataset. **Bold** indicates the best. Underline indicates the second best.

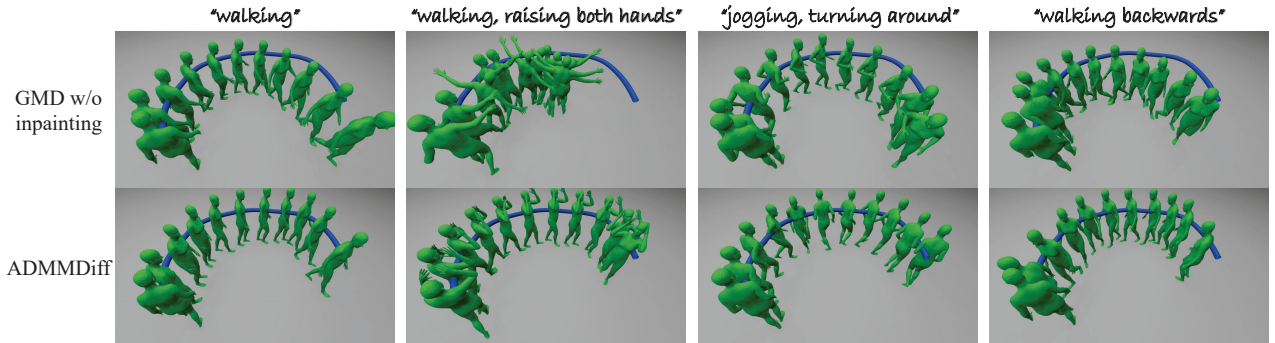


Figure 5. Qualitative comparison on controllable motion generation using trajectory guidance. Blue line indicates the path to follow. The results show that our method better follows the trajectory while being consistent with the motion prior and text prompt.